ACS Energy LETTERS

http://pubs.acs.org/journal/aelccp

LETTER

Understanding Limitations in Electrochemical Conversion to CO at Low CO_2 Concentrations

Danielle A. Henckel, Prantik Saha, Sunil Rajana, Carlos Baez-Cotto, Audrey K. Taylor, Zengcai Liu, Michael G. Resch, Richard I. Masel, and K. C. Neyerlin*

Cite This: *ACS Energy Lett.* 2024, 9, 3433−3439

Read Online

ACCESS | Metrics & More | Article Recommendations | Supporting Information

ABSTRACT: Low-temperature electrochemical CO_2 reduction has demonstrated high selectivity for CO when devices are operated with pure CO_2 streams. However, there is currently a dearth of knowledge for systems operating below 30% CO_2, a regime interesting for coupling electrochemical devices with CO_2 point sources. Here we examine the influence of ionomer chemistry and cell operating conditions on the CO selectivity at low CO_2 concentrations. Utilizing advanced electrochemical diagnostics, values for cathode catalyst layer ionic resistance and electrocatalyst capacitance as a function of relative humidity (RH) were extracted and correlated with selectivity and catalyst utilization. Staying above 20% CO_2 concentration with at least a 50% cathode RH resulted in >95% CO/H_2 selectivity regardless of the ionomer chemistry. At 10% CO_2, however, >95% CO/H_2 selectivity was only obtained at 95% RH under scenarios where the resulting electrode morphology enabled high catalyst utilization.

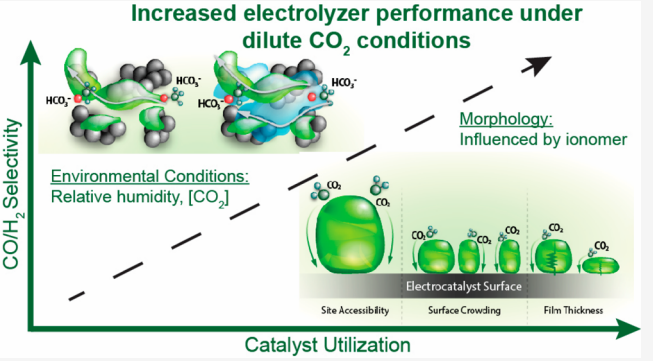

INTRODUCTION

The electrochemical conversion of CO_2 into commodity chemicals is currently being investigated to utilize low-carbon electricity into the chemical industry and upgrade CO_2 into value-added products. Of the available candidate chemicals to be produced electrochemically from CO_2, CO has the largest market price of CO_2 reduction products and technologies for the electrochemical conversion are increasingly mature.[1−4] Since the largest amounts of CO_2 emitted are from industrial sources at less than 30%,[5,6] and the enrichment of CO_2 streams from carbon capture will be cost-intensive, CO_2 to CO at low concentrations of CO_2 could greatly impact industrial decarbonization. To date, most work on CO_2 to CO conversion has focused on pure feed streams of 100% CO_2 and relatively few studies have investigated electrocatalytic activity at low concentrations of CO_2.[7−9]

Currently, CO_2 to CO electrolyzers can run at >95% CO/H_2 selectivity at 200 mA/cm^2 and ≤3 V in a zero gap configuration for greater than 3500 h.[10] This high selectivity for CO_2 to CO can be realized by a zero gap system utilizing the anion exchange ionomer polystyrene 1,2,3,4-tetramethylimidazolium chloride (Sustainion) and an anion exchange membrane incorporating the same imidazolium functionality. In this work, we extend this previous zero gap configuration to focus on CO/H_2 selectivity at low concentrations of CO_2. In order to tackle the decreasing CO selectivity with decreasing CO_2 concentration, other work has focused on catalyst development, water crossover, CO_2 pressure, electrochemical pulsing, and ionomer distribution.[8,9,11,12] In this work, we focus instead on the impact of ionomer chemistry and its resulting influence on the electrode morphology and electrochemical properties to improve CO selectivity at low CO_2 concentrations.

The surface electric field plays an important role in selectivity for the electrochemical reduction of CO_2 and has been suggested to increase the local concentration of CO_2 at the surface by stabilizing negatively charged intermediates and preventing diffusion of H_3O^+, thus synergistically promoting CO_2 reduction over the hydrogen evolution reaction (HER).[13−17] While most work has focused on the role that cations play on the surface electric field of the electrode, this can also be induced by cationic ionomer groups.[18] Utilizing a higher concentration of electrolyte cations and cationic ionomers purportedly suppresses the HER and enables CO_2 reduction at low pH. The same strategy could be effective

Received: May 3, 2024
Revised: June 7, 2024
Accepted: June 14, 2024
Published: June 24, 2024

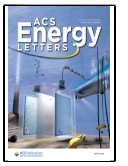

https://doi.org/10.1021/acsenergylett.4c01224
ACS Energy Lett. 2024, 9, 3433−3439

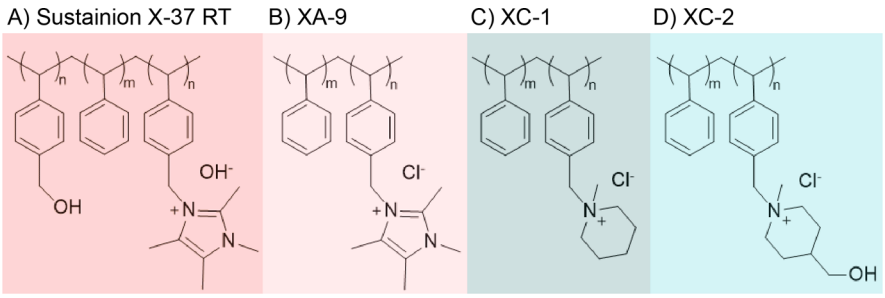

Figure 1. Structures of polymers used in this study: (A) Sustainion X-37 RT (membrane); (B) XA-9; (C) XC-1; (D) XC-2 (ionomer polymers).

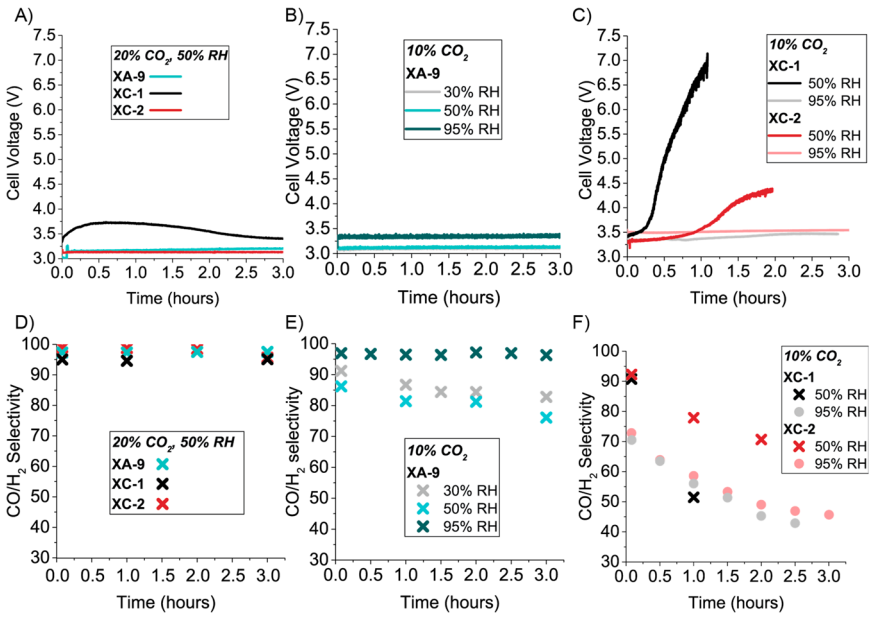

Figure 2. Time versus cell voltage for a 25 cm^2 cell operating at 200 mA/cm^2 for (A) XA-9, XC-1, and XC-2 at 20% CO_2 and 50% RH, (B) XA-9 at 10% CO_2 and 30, 50, and 95% RH, and (C) XC-1 and XC-2 at 10% CO_2 and 50 and 95% RH. (D−F) Corresponding CO/H_2 selectivities for data in (A−C).

when using low concentrations of CO_2, where competition with HER is also a concern. In this study, we explore different cationic group ionomers (imidazolium and piperidinium) that vary in degree of localized charge and hydrophobicity to understand the impact these properties (water transport, stabilization of charged intermediates) have on CO_2 to CO conversion at low CO_2 concentrations. By identifying the underlying ionomer properties that lead to improved performance, we can design more efficient catalyst layers for this reaction.

Characterization of Catalyst Layers. To examine the electrode morphology, we obtained scanning electron microscopy (SEM) images (Figures S2−S4). From these images, we can see similar catalyst agglomerates for the high-resolution images and a similar, smooth coating on the low-resolution images with the Ag catalyst completely covering the gas diffusion media. Additionally, we performed EDS on the electrodes to detect the Cl^- counterion associated with the ionomers. From Figures S5−S7, the Cl^- signal is evenly distributed, demonstrating that, qualitatively, all the ionomers have been well incorporated into the catalyst layers. Nominally a well-distributed ionomer network in the catalyst layer has been attributed to promotion of ion transport pathways.[12] Previous work by Saha et al. identified that cathode ionomer and ions from anolyte crossover equally influence the ionic conductivity in CO_2 cathodes.[19] The function of the ionomer is likely 2-fold; one to facilitate ionic conduction and two to help disperse the catalyst in the ink and influence the resulting electrode morphology.

CO/H_2 Selectivity at Different Concentrations of CO_2. As mentioned in the Introduction, current CO_2 to CO electrolyzers can maintain >95% CO/H_2 selectivity at 200 mA/cm^2, when utilizing 100% CO_2 and operating at 100% relative humidity (RH) feed.[10] In order to understand the effect of the CO_2 concentration and RH on the CO/H_2 selectivity, we tested Ag cathodes utilizing three different ionomers (labeled as XA-9, XC-1, and XC-2, see Figure 1) across a range of different operating conditions. Figure 2A,D show the cell voltage and product selectivity for XA-9, XC-1, and XC-2 under conditions of 20% CO_2 and 50% RH at 200 mA/cm^2. All three ionomers maintain a CO/H_2 selectivity of >95% for 3 h at these conditions. Both the XA-9 and XC-2 electrodes maintain a voltage below 3.3 V, with the XC-1 electrode at a voltage of ∼150 mV higher. While all three electrodes had similar performance at 20% CO_2 and 50% RH, this was not the case when they were operated under more challenging conditions. Figure 2B,E shows the cell voltage and CO/H_2 selectivity for the XA-9 electrode at 10% CO_2 and 30,

https://doi.org/10.1021/acsenergylett.4c01224
ACS Energy Lett. 2024, 9, 3433−3439

50, and 95% RH. From the most challenging experiment of 10% CO_2 with 30% RH, we found that the CO/H_2 selectivity was <90% and continued to drop over 3 h. While increasing the RH to 50% did not improve the selectivity, increasing the RH to 95% allowed the selectivity to remain >95% for 3 h with a stable voltage of ∼3.4 V.

Similar to the XA-9 electrodes at low RH and 10% CO_2, the XC-1 and XC-2 electrodes also had decreased performance, though the voltage increase was exacerbated. The voltage and CO/H_2 selectivity can be seen in Figure 2C,F, respectively, for the XC-1- and XC-2-incorporated electrodes at 10% CO_2 and 50% and 95% RH. As seen in Figure 2C, the voltage profiles for XC-1 and XC-2 increased over time at 10% CO_2 and 50% RH. The cell voltage from the XC-1 electrode increased rapidly to 7 V within the first hour, and the voltage from the XC-2 electrode increased to 4.5 V at the 2 h mark. The CO/H_2 selectivity for the XC-2 electrode decreased to <75% at 2 h and declined even faster for the XC-1 electrodes to ∼50% at 1 h. Notably, the voltage increase for both systems was much larger than expected from anticipated Nernstian voltage change due to a reduced CO_2 concentration (∼9 mV). Suspecting that the increased voltage was the result of restricted ion transport pathways in the catalyst layer,[12] the cell RH was increased to 95%. As seen in Figure 2C, this stabilized the cell voltages for all three electrodes, keeping them below 3.5 V for the duration of the test. However, CO/H_2 selectivity still decreased for both XC-1 and XC-2 electrodes to <50% within 3 h.

From the data set in Figure 2, we uncover two interesting aspects of CO_2 to CO conversion at low CO_2 concentrations under our conditions. First, humidity is an important factor for maintaining a consistent low cell voltage, and second, variations in ionomer composition can impact CO selectivity. Since the selectivity decreases over several hours, and an increase in humidity can mitigate this loss of selectivity in the case of the XA-9 electrode, we hypothesized that the gradual decrease in CO/H_2 selectivity might be due to a decrease in catalyst utilization.[20]

In order to understand the mechanism for increased voltages from XC-1 and XC-2, we performed a voltage recovery experiment (Figure S11). In this experiment (XC-1, 50% RH), we varied the CO_2 concentration from 100% to 10% and the voltage change was instantaneous, increasing from ∼3 to 7 V within 10 min. This voltage change is reversible, and upon raising the CO_2 feed to 100%, the voltage decreased back to the baseline. Due to the instantaneous nature of the voltage response, we consider that the high voltages for XC-1 and XC-2 may be due to a lower concentration of CO_2 throughout the electrode. While the direct interface with the membrane should be wetted for the reaction to occur there, the reaction must move further into the catalyst layer to maintain the same rates under lower reactant conditions. If access to the entire catalyst layer is inhibited through low catalyst utilization, the cell voltage will increase and the selectivity will decrease. The increase in RH stabilized the voltage for XC-1 and XC-2, but still led to a decrease in CO/H_2 selectivity. In this case, the hydrogen evolution reaction (HER) is increasingly preferred, likely due to an increase in the H_2O/CO_2 ratio.

Relative Capacitance as a Function of RH. Electrochemical impedance spectroscopy (EIS) was used to elucidate the maximum available electrochemical surface area as a function of RH. Catalyst utilization describes the fraction of catalyst that is available to the electrochemical reaction (for discussion, see refs 21 and 22).These experiments were performed as previously described (Figure S12).[19] Briefly, we will measure the EIS in a region where no or little charge transfer is occurring. This will allow us to fit our data to a transmission line model and extract the resistance to charge transfer within the catalyst layer.[19] In this configuration, the anode (Pt/C with H_2) serves two purposes: as a reference hydrogen electrode (RHE) and as a counter electrode performing either a hydrogen oxidation reaction (HOR) or hydrogen evolution reaction (HER), depending on the voltage bias. The cathode is still separated from the electrolyte with a membrane, so conditions such as electrolyte crossover are reflective of those during the CO_2R experiments. We varied the RH of the cathode gas inlet and measured the EIS in a potential region where only the double-layer capacitance for Ag dominates (0.85 V vs RHE; this potential is near the open circuit potential of the electrode and is likely due to the presence of oxides on the surface of the Ag). From the EIS, we extracted the capacitance of the electrodes and normalized them to the capacitance at 30% RH (Figure 3A). Interestingly,

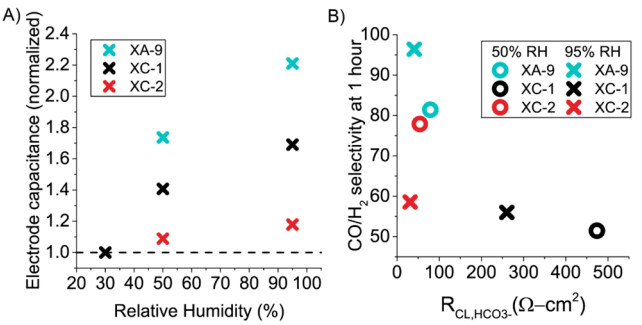

Figure 3. (A) Relative humidity (%) versus normalized electrode capacitance (all values are normalized to capacitance at 30% RH for respective electrodes). (B) Ionic resistance of the catalyst layer (R_{CL,HCO_3^-} (Ω cm^2)) versus CO/H_2 selectivity at 1 h at 200 mA/cm^2 for XA-9, XC-1, and XC-2 at 10% CO_2 and 50% and 95% RH.

all three electrodes had different water uptake properties, with XA-9's capacitance increasing 2.2 times from 30% to 95% RH. In contrast, the XC-1 and XC-2 electrodes have a lower capacitance response to RH, increasing by 1.7 and 1.2 times, respectively. The increase in capacitance as a function of RH is a result of capillary condensation filling pores and providing increased ion conducting pathways. Capillary condensation occurs when the pore vapor pressure or capillary pressure is greater than the water saturation vapor pressure. The vapor pressure inside pores can be greater than the water saturation pressure due to the van der Waals interactions inside the pore. This effect allows water to condense more readily in pores with smaller pore sizes undergoing capillary condensation at lower RH. From the data in Figure 3, we hypothesize that the average capillary pressure is greater in the order XA-9 > XC-1 > XC-2. The average capillary pressure in this system can by influenced by pore size, pore volume, or the surface tension of the intruding liquid (influenced by the additives or surfactants).[20,23,24]

In these systems, water can be provided either by the anolyte (from membrane crossover) or by the cathode feed gas water vapor. Previously, it has been shown that, in Cu electrodes in a similar membrane electrode assembly, an increase in cathode gas RH increased the surface conductivity by 1.5 times from 0 to 100% RH, even with KOH electrolyte present.[19] As seen in

https://doi.org/10.1021/acsenergylett.4c01224
ACS Energy Lett. 2024, 9, 3433−3439

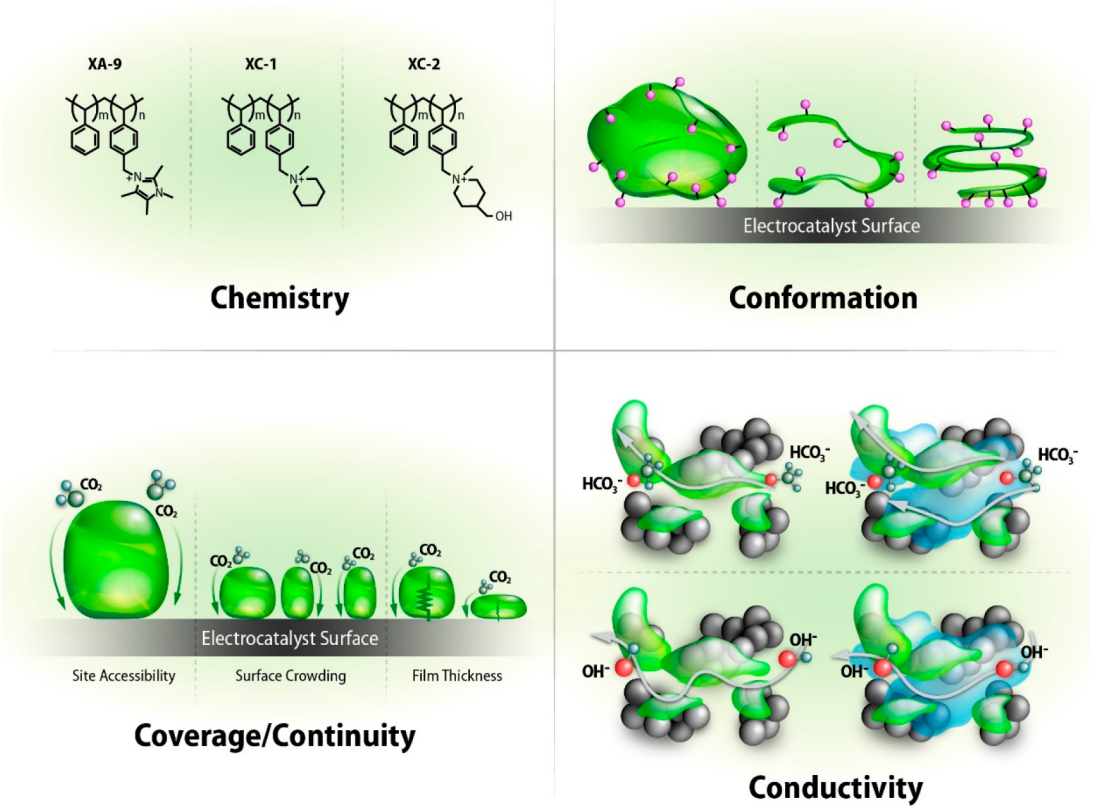

Figure 4. Schematics depicting various ionomer properties (chemistry, confirmation, coverage/continuity, and conductivity) that can impact electrode performance.

Figure 3, the electrode capacitance is influenced by the relative humidity of the gas stream, which demonstrates that the electrodes are not fully wetted by the electrolyte crossover alone. As seen in the performance data for XC-1 and XC-2, the voltage rapidly increases when at 50% RH but is stable at 95% RH. This could be due to a loss of electrode capacitance at lower RHs.

An interesting aspect of this work is that the ionomer appears to influence the water distribution in the catalyst layer. The capillary pressure of pores can be influenced by surfactants, so it is possible that the hydrophobicity of the ionomer can play a role in the difference in average capillary pressure for the electrodes.[23−25] For example, this has been shown in the case of carbon electrodes, where Nafion content increased wetting.[26] The increase in relative electrode capacitance with relative humidity from Figure 3A correlates with the expected hydrophobicity of the ionomers XA-9 > XC-1 > XC-2. The charge-delocalized imidazolium group of the XA-9 ionomer will be more hydrophilic than the piperidinium groups of XC-1 and XC-2.[27] Additionally, the XC-1 ionomer contains a methylhydroxy group, increasing the ionomer's hydrophilicity. While catalyst layer hydrophobicity[28] and increased water in the catalyst layer[12,29] are typically correlated with an increased CO_2R over the HER, in this case an increase in feed gas humidity is increasing the electrode capacitance and therefore catalyst utilization. Additionally, other work with membrane electrode assemblies for CO_2 CO conversion has noted the advantageous role of increased water in the catalyst layer. Kim et al. noted that increased water crossover, through flow rate, increased the FE for CO[9] and work by Wei et al. has demonstrated that increased water in the catalyst layer, through ionomer incorporation, increases the formation of the *COOH intermediate, thereby increasing CO FE.[30] Although other work has described amine-based additives as increasing the local CO_2 concentration in the catalyst layer,[31,32] we do not expect this to be a significant effect due to the lack of a lone pair on the nitrogen in the charged ionomers used in this work.

Ion Transport through the Catalyst Layer. We can also extract the resistance to ion transport (R_{CL,HCO_3^-}) through the catalyst layer from the EIS. A higher resistance to ion transport indicates that the ion transport through the catalyst is inhibited, potentially originating from disconnected ionomer pathways in the catalyst layer[33] or ionomer type.[34] If the catalyst layer has a higher ionic resistance, the effective catalyst surface area will be lower than in the geometric catalyst layer, resulting in an uneven current distribution throughout the electrode.[21]

Resistance to ion transport of HCO_3^- (HCO_3^- is assumed to the charge carrier in this specific measurement due to the low current conditions) versus the CO/H_2 selectivity at 1 h can be seen in Figure 3B. The ionomer XC-1 has a significantly higher R_{CL,HCO_3^-} than the other ionomers by 2 orders of magnitude. This means that the catalyst utilization for XC-1 will be much lower than those for the other electrodes, which is reflected in its lower CO/H_2 selectivity. Relative humidity also has an effect on R_{CL,HCO_3^-} increasing this value by ∼200 Ω cm^2, from 95% to 50% RH for the XC-1 electrode due to increased access within the catalyst layer. The XC-2 electrode has a R_{CL,HCO_3^-} value comparable to that of the XA-9 electrode, <50 Ω cm^2. However, its decreased ability to increase

https://doi.org/10.1021/acsenergylett.4c01224
ACS Energy Lett. 2024, 9, 3433−3439

capacitance as a function of RH may lead to lower catalyst utilization and an increase in R_{CL,HCO_3^-} at longer times (increased voltage in Figure 2C at 2 h). The R_{CL,HCO_3^-} data do not correlate with the ion exchange capacity (IEC) data of the ionomer polymers alone. We measured the IEC of the XA-9, XC-1, and XC-2 ionomer polymers (Table S1), as this could affect the ability of the ionomer to transport charge. Interestingly the XC-1 and XC-2 ionomers have a similar (~1.39 mM/g) ion exchange capacity (IEC), higher than that of XA-9 (0.94 mM/g). We hypothesize that other factors, such as the ionomer polymer conformation, are also playing a role in the ion transport through the catalyst layer.

SUMMARY

In summary, Figure 4 describes the various impacts that ionomers can have on the electrochemical properties of the electrode. The chemistry of the ionomer can affect the hydrophobicity of the catalyst layer, ion conductivity, and reactant gas permeability.[35] The conformation of the ionomer can also be influenced by the catalyst ink[36,37] and deposition[22] method, netting changes in competitive adsorption processes and local gas transport. Significantly thick ionomer films can result in underutilized catalyst sites, where reactant gases are forced around areas with low permeability. Furthermore, changes in ionomer coverage on electrocatalyst sites can influence ionic accessibility to the reaction site, while variations in film thickness influence non-Fickian diffusion resistance.[38] The breadth of electrode level morphological changes that can occur as ionomer chemistry/properties are modified makes it difficult to elucidate and isolate the impact of said modification. Only through close examination of device level electrochemical properties combined with performance and selectivity assessments can one truly unravel the benefit of the proposed material solutions.

This work demonstrated that, beyond ionomer properties, electrode-level electrochemical phenomena affect CO/H_2 selectivity at low CO_2 concentrations. We have identified two important electrode-level parameters that we attribute to differences in ionomer chemistry and/or integration: capacitance increase as a function of RH (related to pore size and/or hydrophobicity) and the resistance of the ion transport (R_{CL,HCO_3^-}) through the catalyst layer. The RH of the cathode feed gas can be an important factor in increasing catalyst utilization, but only if the electrode can distribute water throughout the catalyst layer, which could be influenced by pore size, pore volume, or ionomer hydrophobicity. In scenarios of poor catalyst utilization (low ion transport), electrodes will not have simultaneous access to both gas phase CO_2 and ions, with the HER favored under these conditions. Ion conduction through the catalyst layer is important for maximum catalyst utilization. This utilization will be especially important in mass transport limited regimes, such as at low CO_2 concentrations. In this study we find that these electrode level properties influenced by the ionomer affect the performance of the electrode toward conversion of CO_2 to CO at low concentrations of CO_2. Figure 4 depicts different ionomer properties, such as ionomer chemistry and conformation, potentially leading to the electrode property level observations observed in this study.

The promising results here may also be due to the high loadings of Ag (~3 mg/cm^2), which has been implicated in lowering the neutralized CO_2 in the catalyst layer due to the higher CO_2/OH^- ratio.[7] It is clear that every CO_2 system will have different requirements for optimal performance and we have identified factors that will affect CO_2 to CO in a zero gap system with a dilute anolyte and a high catalyst loading. Future work will focus on understanding the kinetics of the CO_2R and HER on Ag electrodes to maximize performance under low reactant access conditions.

ASSOCIATED CONTENT

Supporting Information

The Supporting Information is available free of charge at https://pubs.acs.org/doi/10.1021/acsenergylett.4c01224.

Detailed experimental methods, scanning electron microscopy images and electrochemical impedance spectra (PDF)

AUTHOR INFORMATION

Corresponding Author

K. C. Neyerlin − *National Renewable Energy Laboratory, Golden, Colorado 80401, United States;* orcid.org/0000-0002-6753-9698; Email: Kenneth.neyerlin@nrel.gov

Authors

Danielle A. Henckel − *National Renewable Energy Laboratory, Golden, Colorado 80401, United States;* orcid.org/0000-0003-2640-7127

Prantik Saha − *National Renewable Energy Laboratory, Golden, Colorado 80401, United States;* orcid.org/0000-0001-9417-6872

Sunil Rajana − *Dioxide Materials, Boca Raton, Florida 33487, United States*

Carlos Baez-Cotto − *National Renewable Energy Laboratory, Golden, Colorado 80401, United States*

Audrey K. Taylor − *National Renewable Energy Laboratory, Golden, Colorado 80401, United States;* orcid.org/0000-0003-0985-5120

Zengcai Liu − *Dioxide Materials, Boca Raton, Florida 33487, United States*

Michael G. Resch − *National Renewable Energy Laboratory, Golden, Colorado 80401, United States*

Richard I. Masel − *Dioxide Materials, Boca Raton, Florida 33487, United States*

Complete contact information is available at: https://pubs.acs.org/10.1021/acsenergylett.4c01224

Notes

The authors declare the following competing financial interest(s): Dioxide Materials has patented and is selling the membranes and ionomers tested in this paper. R.I.M. and Z.L. have an interest in these materials.

ACKNOWLEDGMENTS

This work was funded by the Bio Energy Technology Office, authored in part by Alliance for Sustainable Energy, LLC, the manager, and operator of the National Renewable Energy Laboratory for the U.S. Department of Energy (DOE) under Contract No. DE-AC36-08GO28308. The authors would like to thank Ellis Klein, Cole Delery, Jacob McCloud, and Holly Gadpaille for their technical support and equipment maintenance. The views expressed in the article do not necessarily represent the views of the DOE or the U.S. Government. The U.S. Government retains and the publisher,

REFERENCES

(1) Masel, R. I.; Liu, Z.; Yang, H.; Kaczur, J. J.; Carrillo, D.; Ren, S.; Salvatore, D.; Berlinguette, C. P. An Industrial Perspective on Catalysts for Low-Temperature CO2 Electrolysis. *Nat. Nanotechnol.* **2021**, *16* (2), 118−128.
(2) Weekes, D. M.; Salvatore, D. A.; Reyes, A.; Huang, A.; Berlinguette, C. P. Electrolytic CO2 Reduction in a Flow Cell. *Acc. Chem. Res.* **2018**, *51* (4), 910−918.
(3) Jin, S.; Hao, Z.; Zhang, K.; Yan, Z.; Chen, J. Advances and Challenges for the Electrochemical Reduction of CO2 to CO: From Fundamentals to Industrialization. *Angew. Chem., Int. Ed.* **2021**, *60* (38), 20627−20648.
(4) Krause, R.; Reinisch, D.; Reller, C.; Eckert, H.; Hartmann, D.; Taroata, D.; Wiesner-Fleischer, K.; Bulan, A.; Lueken, A.; Schmid, G. Industrial Application Aspects of the Electrochemical Reduction of CO2 to CO in Aqueous Electrolyte. *Chemie Ingenieur Technik* **2020**, *92* (1−2), 53−61.
(5) Wang, X.; Song, C. Carbon Capture From Flue Gas and the Atmosphere: A Perspective. *Frontiers in Energy Research* **2020**, *8*, 1−24.
(6) Last, G. V.; Schmick, M. T. A Review of Major Non-Power-Related Carbon Dioxide Stream Compositions. *Environ. Earth Sci.* **2015**, *74* (2), 1189−1198.
(7) Xu, Q.; Xu, A.; Garg, S.; Moss, A. B.; Chorkendorff, I.; Bligaard, T.; Seger, B. Enriching Surface-Accessible CO2 in the Zero-Gap Anion-Exchange-Membrane-Based CO2 Electrolyzer. *Angew. Chem., Int. Ed.* **2023**, *62* (3), No. e202214383.
(8) Kim, B.; Ma, S.; Molly Jhong, H.-R.; Kenis, P. J. A. Influence of Dilute Feed and PH on Electrochemical Reduction of CO2 to CO on Ag in a Continuous Flow Electrolyzer. *Electrochim. Acta* **2015**, *166*, 271−276.
(9) Kim, D.; Choi, W.; Lee, H. W.; Lee, S. Y.; Choi, Y.; Lee, D. K.; Kim, W.; Na, J.; Lee, U.; Hwang, Y. J.; et al. Electrocatalytic Reduction of Low Concentrations of CO2 Gas in a Membrane Electrode Assembly Electrolyzer. *ACS Energy Letters* **2021**, *6* (10), 3488−3495.
(10) Liu, Z.; Yang, H.; Kutz, R.; Masel, R. I. CO2 Electrolysis to CO and O2 at High Selectivity, Stability and Efficiency Using Sustainion Membranes. *J. Electrochem. Soc.* **2018**, *165* (15), J3371.
(11) Van Daele, S.; Hintjens, L.; Van den Hoek, J.; Neukermans, S.; Daems, N.; Hereijgers, J.; Breugelmans, T. Influence of the Target Product on the Electrochemical Reduction of Diluted CO2 in a Continuous Flow Cell. *Journal of CO2 Utilization* **2022**, *65*, 102210.
(12) Du, X.; Zhang, P.; Zhang, G.; Gao, H.; Zhang, L.; Zhang, M.; Wang, T.; Gong, J. Confinement of Ionomer for Electrocatalytic CO2 Reduction Reaction via Efficient Mass Transfer Pathways. *National Science Review* **2024**, *11*, nwad149.
(13) Gu, J.; Liu, S.; Ni, W.; Ren, W.; Haussener, S.; Hu, X. Modulating Electric Field Distribution by Alkali Cations for CO2 Electroreduction in Strongly Acidic Medium. *Nat. Catal* **2022**, *5* (4), 268−276.
(14) Ringe, S.; Morales-Guio, C. G.; Chen, L. D.; Fields, M.; Jaramillo, T. F.; Hahn, C.; Chan, K. Double Layer Charging Driven Carbon Dioxide Adsorption Limits the Rate of Electrochemical Carbon Dioxide Reduction on Gold. *Nat. Commun.* **2020**, *11* (1), 33.
(15) Ringe, S.; Clark, E. L.; Resasco, J.; Walton, A.; Seger, B.; Bell, A. T.; Chan, K. Understanding Cation Effects in Electrochemical CO2 Reduction. *Energy Environ. Sci.* **2019**, *12* (10), 3001−3014.
(16) Lee, M.-Y.; Ringe, S.; Kim, H.; Kang, S.; Kwon, Y. Electric Field Mediated Selectivity Switching of Electrochemical CO2 Reduction from Formate to CO on Carbon Supported Sn. *ACS Energy Lett.* **2020**, *5* (9), 2987−2994.
(17) Chen, L. D.; Urushihara, M.; Chan, K.; Nørskov, J. K. Electric Field Effects in Electrochemical CO2 Reduction. *ACS Catal.* **2016**, *6* (10), 7133−7139.
(18) Fan, M.; Huang, J. E.; Miao, R. K.; Mao, Y.; Ou, P.; Li, F.; Li, X.-Y.; Cao, Y.; Zhang, Z.; Zhang, J.; Yan, Y.; Ozden, A.; Ni, W.; Wang, Y.; Zhao, Y.; Chen, Z.; Khatir, B.; O'Brien, C. P.; Xu, Y.; Xiao, Y. C.; Waterhouse, G. I. N.; Golovin, K.; Wang, Z.; Sargent, E. H.; Sinton, D. Cationic-Group-Functionalized Electrocatalysts Enable Stable Acidic CO2 Electrolysis. *Nat. Catal* **2023**, *6*, 763.
(19) Saha, P.; Henckel, D.; Intia, F.; Hu, L.; Cleve, T. V.; Neyerlin, K. C. Anolyte Enhances Catalyst Utilization and Ion Transport Inside a CO2 Electrolyzer Cathode. *J. Electrochem. Soc.* **2023**, *170* (1), 014505.
(20) Cetinbas, F. C.; Ahluwalia, R. K.; Kariuki, N. N.; Andrade, V. D.; Myers, D. J. Effects of Porous Carbon Morphology, Agglomerate Structure and Relative Humidity on Local Oxygen Transport Resistance. *J. Electrochem. Soc.* **2019**, *167* (1), 013508.
(21) Neyerlin, K.; Gu, W.; Jorne, J.; Clark, A.; Gasteiger, H. A. Cathode Catalyst Utilization for the ORR in a PEMFC: Analytical Model and Experimental Validation. *J. Electrochem. Soc.* **2007**, *154* (2), B279.
(22) Henckel, D.; Saha, P.; Intia, F.; Taylor, A. K.; Baez-Cotto, C.; Hu, L.; Schellekens, M.; Simonson, H.; Miller, E. M.; Verma, S.; Mauger, S.; Smith, W. A.; Neyerlin, K. C. Elucidation of Critical Catalyst Layer Phenomena toward High Production Rates for the Electrochemical Conversion of CO to Ethylene. *ACS Appl. Mater. Interfaces* **2024**, *16* (3), 3243−3252.
(23) Fujita, S.; Koiwai, A.; Kawasumi, M.; Inagaki, S. Enhancement of Proton Transport by High Densification of Sulfonic Acid Groups in Highly Ordered Mesoporous Silica. *Chem. Mater.* **2013**, *25* (9), 1584−1591.
(24) Brumaru, C.; Geng, M. L. Interaction of Surfactants with Hydrophobic Surfaces in Nanopores. *Langmuir* **2010**, *26* (24), 19091−19099.
(25) Yan, X.-M.; Mei, P.; Mi, Y.; Gao, L.; Qin, S. Proton Exchange Membrane with Hydrophilic Capillaries for Elevated Temperature PEM Fuel Cells. *Electrochem. Commun.* **2009**, *11* (1), 71−74.
(26) Soboleva, T.; Malek, K.; Xie, Z.; Navessin, T.; Holdcroft, S. PEMFC Catalyst Layers: The Role of Micropores and Mesopores on Water Sorption and Fuel Cell Activity. *ACS Appl. Mater. Interfaces* **2011**, *3* (6), 1827−1837.
(27) Freire, M. G.; Neves, C. M. S. S.; Carvalho, P. J.; Gardas, R. L.; Fernandes, A. M.; Marrucho, I. M.; Santos, L. M. N. B. F.; Coutinho, J. A. P. Mutual Solubilities of Water and Hydrophobic Ionic Liquids. *J. Phys. Chem. B* **2007**, *111* (45), 13082−13089.
(28) Li, M.; Idros, M. N.; Wu, Y.; Burdyny, T.; Garg, S.; Zhao, X. S.; Wang, G.; Rufford, T. E. The Role of Electrode Wettability in Electrochemical Reduction of Carbon Dioxide. *Journal of Materials Chemistry A* **2021**, *9* (35), 19369−19409.
(29) Reyes, A.; Jansonius, R. P.; Mowbray, B. A. W.; Cao, Y.; Wheeler, D. G.; Chau, J.; Dvorak, D. J.; Berlinguette, C. P. Managing Hydration at the Cathode Enables Efficient CO2 Electrolysis at Commercially Relevant Current Densities. *ACS Energy Lett.* **2020**, *5* (5), 1612−1618.
(30) Wei, P.; Li, H.; Li, R.; Wang, Y.; Liu, T.; Cai, R.; Gao, D.; Wang, G.; Bao, X. The Role of Interfacial Water in CO2 Electrolysis over Ni-N-C Catalyst in a Membrane Electrode Assembly Electrolyzer. *Small* **2023**, *19* (25), 2300856.
(31) Chen, X.; Chen, J.; Alghoraibi, N. M.; Henckel, D. A.; Zhang, R.; Nwabara, U. O.; Madsen, K. E.; Kenis, P. J.; Zimmerman, S. C.; Gewirth, A. A. Electrochemical CO2-to-Ethylene Conversion on Polyamine-Incorporated Cu Electrodes. *Nature Catalysis* **2021**, *4* (1), 20−27.
(32) Chen, B.; Rong, Y.; Li, X.; Sang, J.; Wei, P.; An, Q.; Gao, D.; Wang, G. Molecular Enhancement of Direct Electrolysis of Dilute CO2. *ACS Energy Lett.* **2024**, *9* (3), 911−918.
(33) Lefebvre, M. C.; Martin, R. B.; Pickup, P. G. Characterization of Ionic Conductivity Profiles within Proton Exchange Membrane

Fuel Cell Gas Diffusion Electrodes by Impedance Spectroscopy. *Electrochem. Solid-State Lett.* **1999**, *2* (6), 259−261.
(34) Jinnouchi, R.; Kudo, K.; Kodama, K.; Kitano, N.; Suzuki, T.; Minami, S.; Shinozaki, K.; Hasegawa, N.; Shinohara, A. The Role of Oxygen-Permeable Ionomer for Polymer Electrolyte Fuel Cells. *Nat. Commun.* **2021**, *12* (1), 4956.
(35) Kongkanand, A.; Mathias, M. F. The Priority and Challenge of High-Power Performance of Low-Platinum Proton-Exchange Membrane Fuel Cells. *J. Phys. Chem. Lett.* **2016**, *7* (7), 1127−1137.
(36) Van Cleve, T.; Khandavalli, S.; Chowdhury, A.; Medina, S.; Pylypenko, S.; Wang, M.; More, K. L.; Kariuki, N.; Myers, D. J.; Weber, A. Z.; Mauger, S. A.; Ulsh, M.; Neyerlin, K. C. Dictating Pt-Based Electrocatalyst Performance in Polymer Electrolyte Fuel Cells, from Formulation to Application. *ACS Appl. Mater. Interfaces* **2019**, *11* (50), 46953−46964.
(37) Mowbray, B. A. W.; Dvorak, D. J.; Taherimakhsousi, N.; Berlinguette, C. P. How Catalyst Dispersion Solvents Affect CO2 Electrolyzer Gas Diffusion Electrodes. *Energy Fuels* **2021**, *35* (23), 19178−19184.
(38) Weber, A. Z.; Kusoglu, A. Unexplained Transport Resistances for Low-Loaded Fuel-Cell Catalyst Layers. *J. Mater. Chem. A* **2014**, *2* (41), 17207−17211.

https://doi.org/10.1021/acsenergylett.4c01224
ACS Energy Lett. 2024, 9, 3433−3439